NUMERICAL SIMULATION OF WALL TEMPERATURE ON GAS PIPELINE DUE TO RADIATION OF NATURAL GAS DURING COMBUSTION

by

Marko N. ILIĆ**, *Velimir P. STEFANOVIĆ*, *Gradimir S. ILIĆ*, *Saša R. PAVLOVIĆ*, *and Dragan D. KUŠTRIMOVIĆ

Faculty of Mechanical Engineering, University of Niš, Niš, Serbia

Original scientific paper
DOI: 10.2298/TSCI120503192I

This paper presents one of the possible hazardous situations during transportation of gas through the international pipeline. It describes the case when at high-pressure gas pipeline, due to mechanical or chemical effect, cracks and a gas leakage appears and the gas is somehow triggered to burn. As a consequence of heat impingement on the pipe surface, change of material properties (decreasing of strength) at high temperatures will occur. In order to avoid greater rapture a reasonable pressure relief rate needs to be applied. Standards in this particular domain of depressurizing procedure are not so exact (DIN EN ISO 23251; API 521). This paper was a part of the project to make initial contribution in defining the appropriate procedure of gas operator behaving during the rare gas leakage and burning situations on pipeline network. The main part of the work consists of two calculations. The first is the numerical simulation of heat radiation of combustible gas, which affects the pipeline, done in the FLUENT software. The second is the implementation of obtained results as a boundary condition in an additional calculation of time resolved wall temperature of the pipe under consideration this temperature depending on the incident flux as well as a number of other heat flow rates, using the Matlab. Simulations were done with the help of the "E.ON Ruhrgas AG" in Essen.

Key words: *sonic release, steady computational fluid dynamics, non-premixed combustion, gas jet thermal reach*

Introduction

Within natural gas processing plants such as compressor stations, the piping is partially located above the ground. In the rare incident of a gas leakage on these high-pressure facilities, a supersonic compressible gas (CH_4) jet will form. This jet may ignite and burn, causing a considerable radiation heat flow rate impinging on the surface of aboveground pipes located in the vicinity of the leak. As a consequence of heat impingement on the pipe surface, change of material properties (decreasing of strength) at high temperatures will occur. In order to avoid greater rapture, a reasonable pressure relief rate needs to be applied. The main goal is the numerical calculation of the radiation heat flux of burning gas jet on the surface of the pipe with the computational fluid dynamics (CFD) software package FLUENT. Achieved results will be

* Corresponding author; e-mail: marko_il@hotmail.com

used as a boundary condition in an additional calculation of time resolved wall temperature of the pipe under consideration, this temperature depending on the incident flux, as well as a number of other heat flow rates. In that direction, further and more exact conclusions about the relieving time will be defined in the future for this specific case. Standards [1] and [2**]** in this particular domain of depressurizing procedure are not so exact, they just state that depressurizing the system should most likely be done within 15 minutes, without giving the reasons why.

Physical and mathematical model of numerical simulation

The assumed parameters in this case were: diameter of pipe 900 mm, wall thickness of 20 mm. Pressure inside the pipe 70 bar, with ambient pressure as pressure outside. Similarly, to the scenario described in [3] it was assumed that the size of the orifice was 100 mm^2. It is known that for a pressure of 70 bar inside the pipe, a compressible, supersonic jet will form. At this pressure the jet expands immediately upstream of the orifice to equilibrate with ambient conditions, as shown in fig. 1. The difficulties associated with solving compressible flows in FLUENT are a result of the high degree of coupling between the flow velocity, density, pressure, and energy. This coupling may lead to instabilities in the solution process and, therefore, may require special solution techniques in order to obtain a converged numerical solution [4]. In addition, the presence of shocks (discontinuities) in the flow introduces an additional stability problem during the calculation.

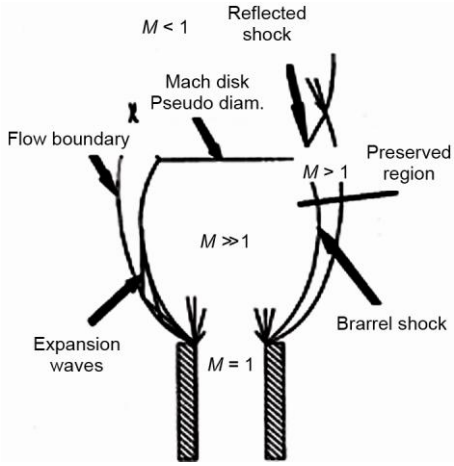

Figure 1. Principal characteristics of the expansion process for an underexpanded jet [5]

Hence a supercritical jet could be expected to behave in a manner analogous to a classical free jet, although with modified velocity and length scales. To reduce the complexity of the problem, *i. e.* to avoid the necessity of modeling a compressible flow in conjunction with combustion and radiation models, the properties of the gas jet after its expansion to a pressure at ambient level are used as an inlet boundary condition of the 3-D simulation. Birch et al. (1984) [5, 6] define a "pseudo-diameter" in figs. 1 and 2, which, when substituted into equations defining a subsonic round free jet, reproduced the observed concentration field in the self preserving region of supercritical methane releases.

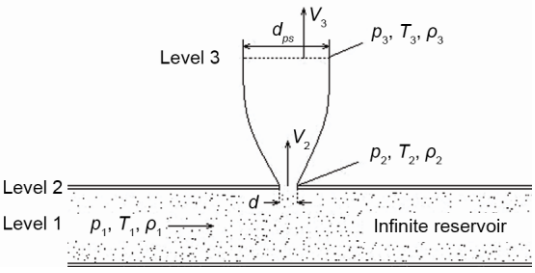

Figure 2. Expanding gas jet [6]

This pseudo diameter in fig. 2 is developed by considering the area which would be occupied by the same mass flow rate at ambient pressure and temperature with a uniform sonic velocity. The present analysis aims to produce an alternative definition according to [5, 6], which conserves both mass and momentum through the expansion region, while retaining the assumption that the pressure is reduced to the ambient level:

– Level 1 – the conditions inside the reservoir temperature,
– Level 2 – the conditions at the orifice, and
– Level 3 – the conditions after the expansion.

Conservation equations for supercritical gas release can be found in [5]. All initial properties for this simulation are derived from these equations in [5, 6].

The general scalar transport equations solved by FLUENT are shown below as RANS model.

– *the mass conservation equation [4]*

$$\frac{\partial \rho}{\partial t} + \nabla(\rho \vec{\mathrm{v}}) = S_m \tag{1}$$

The source S_m is the mass added to the continuous phase from the dispersed second phase (*e. g*. due to vaporization of liquid droplets) or other sources.

– *momentum conservation equations [4]*

$$\frac{\partial(\rho \vec{\mathrm{v}})}{\partial t} + \nabla(\rho \vec{\mathrm{v}}\vec{\mathrm{v}}) = -\nabla p + \nabla(\boldsymbol{\tau}) + \rho\vec{\mathrm{g}} + \vec{\mathrm{F}} \tag{2}$$

where p is the static pressure, $\boldsymbol{\tau}$ – the stress tensor, and $\rho\vec{\mathrm{g}}, \vec{\mathrm{F}}$ are the gravitational body force and external body forces. $\vec{\mathrm{F}}$ also contains other model-dependent source terms such as porous-media and user defined sources.

$$\boldsymbol{\tau} = \mu\left[(\nabla\vec{\mathrm{v}} + \nabla\vec{\mathrm{v}}^T) - \frac{2}{3}\nabla\vec{\mathrm{v}}\mathbf{I}\right] \tag{3}$$

where μ is the molecular viscosity, and $\mathbf{I}$ – the unit tensor.

– *The energy equation for the non premixed combustion model [4]:*

FLUENT solves the total enthalpy form of the energy equation:

$$\frac{\partial(\rho H)}{\partial t} + \nabla(\rho \vec{\mathrm{v}} H) = \nabla\left(\frac{k_t}{c_p}\nabla H\right) + S_h \tag{4}$$

Total enthalpy H is defined as:

$$H = \sum_j Y_j H_j \tag{5}$$

where Y_j is the mass fraction of species j and the total amount of generated heat is the sum of heats generated on active surfaces:

$$H_j = \int_{T_{ref,j}}^{T} c_{p,j}\mathrm{d}T + h_j^0(T_{ref,j}) \tag{4}$$

where $h_j^0(T_{ref,j})$ is the formation enthalpy of species j at the reference temperature $T_{ref,j}$.

The process of combustion is modeled for non-premixed combustion with a mixture fraction approach being based on a probability density function (PDF). The basis of the non premixed modeling approach is that, under a certain set of simplifying assumptions, the instantaneous thermochemical state of the fluid is related to a conserved scalar quantity known as the mixture fraction *f*.

– *Transport equation for the mixture fraction f [4]*

$$\frac{\partial(\rho\overline{f})}{\partial t}+\nabla(\rho\vec{v}\overline{f})=\nabla\left(\frac{\mu_t}{\sigma_t}\nabla\overline{f}\right)+S_m+S_{user} \tag{7}$$

The source term S_m is due solely to transfer of mass into the gas phase from liquid fuel droplets or reacting particles (*e. g.* coal).

In addition to solving for the Favre mean mixture fraction, FLUENT solves a conservation equation for the mixture fraction variance, f^2 (*f* prime square):

$$\frac{\partial(\rho\overline{f^2})}{\partial t}+\nabla(\rho\vec{v}\overline{f^2})=\nabla\left(\frac{\mu_t}{\sigma_t}\nabla\overline{f^2}\right)+C_g\mu_t(\nabla\overline{f})^2-C_d\rho\frac{\varepsilon}{k}\overline{f'^2}+S_{user} \tag{8}$$

where $f'=f-\overline{f}$. The default values for the constants σ_t, C_g, and C_d are 0.85, 2.86, and 2.0, respectively. The mixture fraction variance is used in the closure model describing turbulence – chemistry interactions.

Turbulent viscosity is determined with the two-equation *k-ε* turbulent model for the purpose of the presented reactive flow modeling. The application of *k-ε* turbulent model in the modeling of reactive-flows has been proven by many authors as very successful. Turbulent viscosity is computed combining k and ε as follows:

$$\mu_t=\rho C_\mu\frac{k^2}{\varepsilon} \tag{9}$$

where C_μ is a constant.

Turbulence kinetic energy [4], *k*, and its rate of dissipation, *ε*, are obtained from the transport equations:

$$\frac{\partial(\rho k)}{\partial t}+\frac{\partial(\rho k v_i)}{\partial x_i}=\frac{\partial}{\partial x_i}\left[\left(\mu+\frac{\mu_t}{\sigma_k}\right)\frac{\partial k}{\partial x_j}\right]+G_k+G_b-\rho\varepsilon-Y_M+S_k \tag{10}$$

$$\frac{\partial(\rho\varepsilon)}{\partial t}+\frac{\partial(\rho\varepsilon v_i)}{\partial x_i}=\frac{\partial}{\partial x_i}\left[\left(\mu+\frac{\mu_t}{\sigma_\varepsilon}\right)\frac{\partial\varepsilon}{\partial x_j}\right]+C_1\frac{\varepsilon}{k}(G_k+C_3G_b)-C_{2\varepsilon}\rho\frac{\varepsilon^2}{k}+S_\varepsilon \tag{11}$$

In these equations, G_k represents the generation of turbulence kinetic energy due to the mean velocity gradients. G_b is the generation of turbulence kinetic energy due to buoyancy. $C_{1\varepsilon}$, $C_{2\varepsilon}$, and $C_{3\varepsilon}$ are constants. σ_k and σ_ε are the turbulent Prandtl numbers for *k* and *ε*, respectively. S_k and S_ε are user-defined source terms. $C_{1\varepsilon}$ = 1.44, $C_{2\varepsilon}$ = 1.92, C_μ = 0.09, σ_k = 1.0, and σ_ε = 1.3.

– *Radiation model*

The radiation model was the discrete ordinate method (DOM) for calculating the radiative heat of burning gas jet.

– *The DO model* [4] considers the radiative transfer equation (RTE) in the direction $\vec{s}$ as a field equation. Thus, the equation is written as:

$$\nabla\ I(\vec{r},\vec{s})\vec{s}\ +(a+\sigma_s)I(\vec{r},\vec{s})=an^2\frac{\sigma T^4}{\pi}+\frac{\sigma_s}{4\pi}\int_0^{4\pi}I(\vec{r},\vec{s}')\phi(\vec{s},\vec{s}')\mathrm{d}\Omega' \tag{12}$$

where $\vec{s}$ is the vector of solid angles in the Cartesian system (x, y, z). The DO model solves for as many transport equations as there are directions $\vec{s}$ or solid angles. In this paper 10×10 solid angles and 10×10 pixels are implemented.

Geometry, mashing, and boundary conditions

The simulation was performed on a rectangular computational domain with the edge of 87 m in height and 40 m in length. The parallelepiped had one face located on the ground while the other faces were interfaces to the ambient air. The pipe and pseudo-orifice were as placed in the center, 3 m above the ground surface, the direction of the exiting jet being vertical. In order to obtain quantitatively correct results [7], the second order upwind scheme discretization of the governing equations was used throughout the investigation. On the ground, the standard stagnation condition was imposed. The ground surface was assumed to be hydraulically smooth in order not to mix dispersion effects with surface roughness effects. Surface mash of the domain was triangular and created in Gambit software, with seizing function 1.15 from pipe to the ends. 3-D grid was generated in the T-Grid software and was tetrahedral. The number of cells was 526125.

At the air-to-air boundaries the so-called far field boundary condition was imposed. This condition is applicable when the flow at the domain boundaries is not affected by phenomena that occur inside the computational domain. Particularly this correlates to generated heat during combustion of a gas jet, it has to leave the computational domain when approaches the boundaries. The exit pseudo diameter was d_{ps} = 47.3 mm, the mass flux was kept constant at $\dot{m}$ = 1,26 kg/s. Figures 3 and 4 show geometry of domain and orifice. Components in fig. 3(a) are: 1 – air inlet, 2 – pipe, 3 – gas jet (flame), 4 – computational domain, 5 – pressure outlet, and 6 – transparent boundaries of computational domain. Implemented initial parameters in simulation are: gas-pure methane (CH_4), p_1 = 70 bar, T_1 = 288.15 K, d_2 = 11.28 mm, p_2 = 1 bar, and Poisson coefficient χ = 1.35.

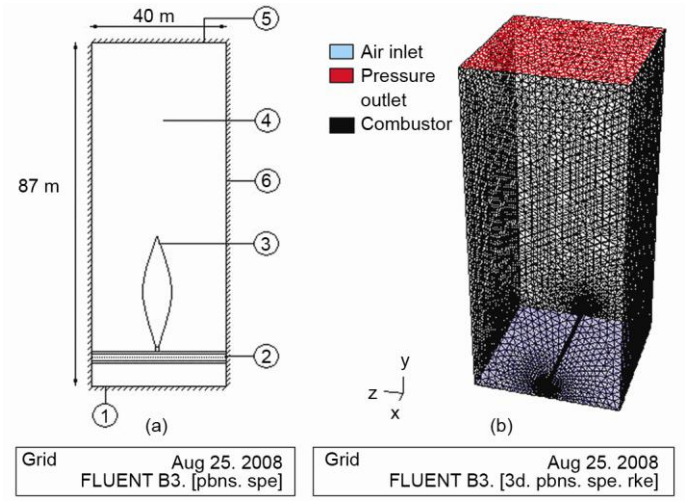

Figure 3. Computational domain; (a) description of domain, (b) mashed domain

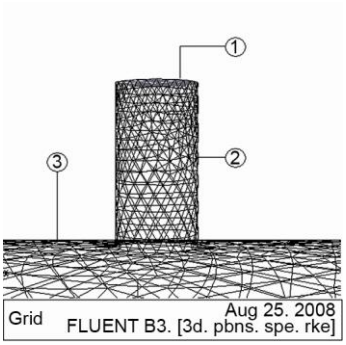

Figure 4. Pseudo orifice gas inlet

In fig. 4, notation 1 is the pseudo orifice (diameter), 2 – the fictive enclosure with growing triangular mesh, and 3 – the triangular mesh of the pipe surface. The simulation was run on 4 processor workstations equipped with 1.8 GHz RISC-CPUs. The simulation of the burning gas jet required about 7 days of CPU time.

Numerical results

After calculating the fully developed burning gas jet with the radiation process, the following figures present the numerical results. Figure 5 shows contour plots of total velocity of the burning gas.

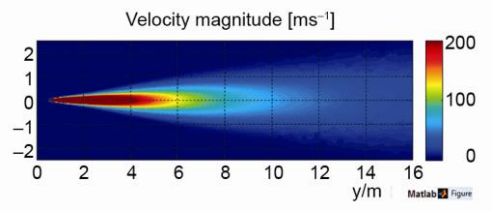

Figure 5. Absolute velocity of burning gas from the pseudo orifice [m/s]

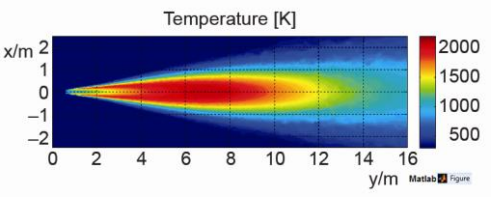

Figure 6. Absolute temperature K of burning gas, at different heights from the orifice

The following figures present the distribution of radiative heat flux on the surface of the pipe $\dot{q}''_F$.

Theoretically, the center part of the pipe in the vicinity of the orifice is the most fragile to further damage (explosion) because of acquired radiation 9 kW/m^2. Further away from the orifice the intensity of the radiation decreases up to 0.3 kW/m^2.

Simplified analytical model

Exposure of the pipe to a fire [8] involves several independent units (the fire, the wall of the pipe, the gas (medium) inside the pipe, the vent and the surroundings). The units are interconnected by appropriate heat, mass and momentum fluxes, as shown below. Heat from the fire is transferred through the wall of the pipe to the gas inside, depending on the nature of the fire. Heat transfer from the flame to the wall region is largely by radiation. Heat may also be transferred from the wall of the pipe to the surroundings or to external cooling.

The middle section of the pipe acquires the highest level of radiative heat, it is in range of 9 kW/m^2 as it is shown in figs. 7-8.

The determination of heat transfer through the wall of the pipe or vessel to the fluid contents requires a complete solution of the transient three dimensional (radial and circumferential) heat conduction equation. This is not trivial. Because the numerical solution can involve significant quantities of computer time, approximations can sometimes be made which reduce the dimensionality of the problem. The basic geometry is essentially cylindrical, and it is tempting to suppose that a full three dimensional analysis of heat transfer through the wall is not needed and simplifying the heat transfer connections from the fig. 9.

In the first case, for simplification, we will assume that the heat flux to the entire vessel is uniform and constant. Thus the important parts of heat transfer are radial conduction to the gas in the pipe, circumferential conduction, and axial conduction as presented in fig. 10. These are closely coupled, but are considered separately for the time being. The driving force

for both axial and circumferential conduction along the wall is small, as well as radiation and convection from the pipe wall to the surrounding area, particularly if the assumption of uniform and constant heat flux is true.

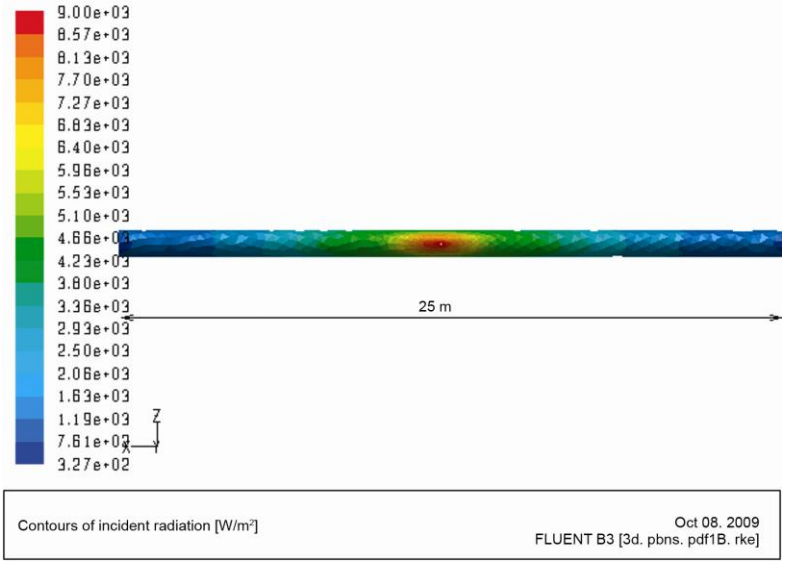

Figure 7. Contours of incident radiation on the pipe (top-bottom view)

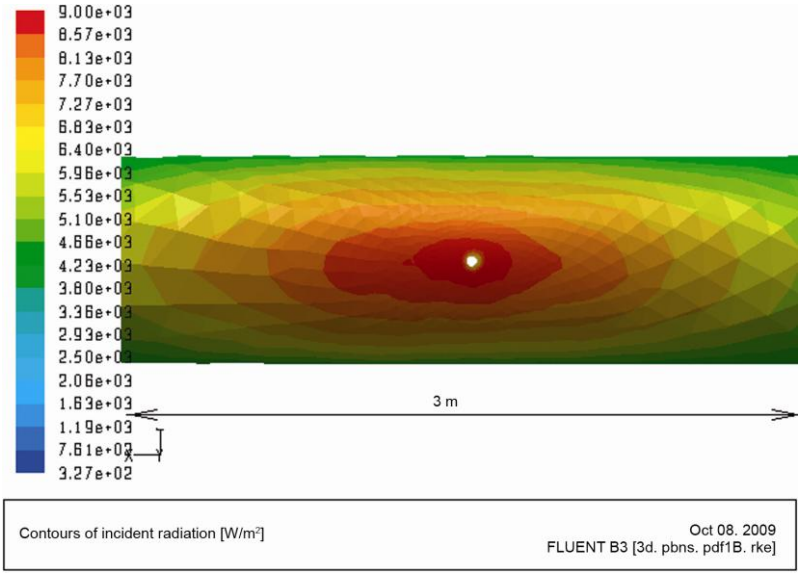

Figure 8. Distribution of radiation on the pipe close to the orifice (top-bottom view)

A useful simplification is to treat the heat transfer just in radial direction, perpendicular to the gas flow. This assumption will give small errors. Heat transfer for the pipe systems where high pressure is present, from the pipe wall to the gas region is largely by convection rather

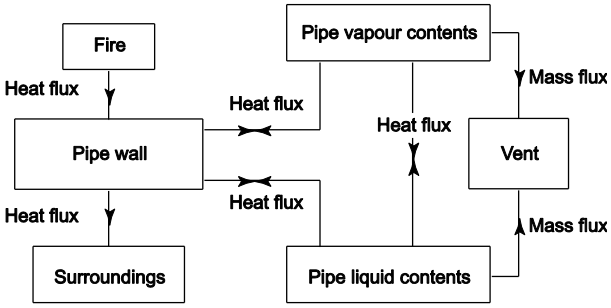

Figure 9. Balance connections between fire, pipe, and gas

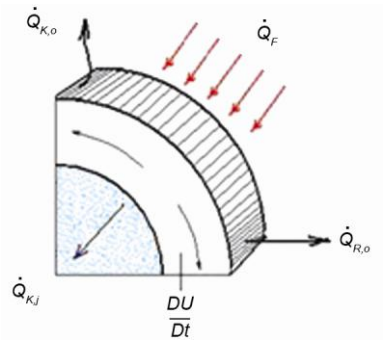

Figure 10. Heat balance for the unit part of the pipe

than the radiation. Although this should be assumed very carefully, because in the cases where medium flow is not present the dominate heat transfer is by radiation, in this situation it is adopted that the pressure inside the pipe is 70 bar and convection prevails the radiation.

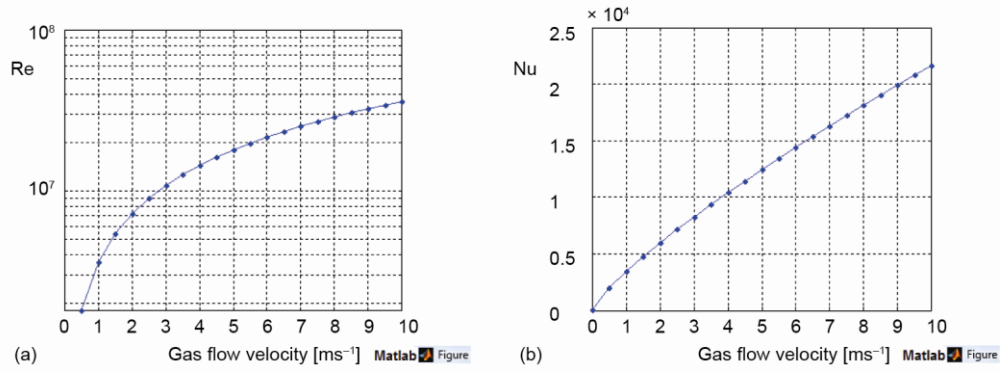

Figure 11. (a) Change of Re, over gas velocity, (b) change of Nu, over gas velocity

The convective flux cannot be determined using an exact theory. Instead, empirical correlations have to be used, generally leading to heat transfer coefficient and hence to the heat flux. Figures 11(a) and (b) show influence in the determination of convective heat transfer coefficient inside the pipe depending on the gas velocity.

The change rate of the internal energy over time is defined by the first law of thermodynamics implemented on a heat transfer [9]:

$$\frac{\mathrm{d}U}{\mathrm{d}t} = \rho_{\mathrm{pipe}} c_{\mathrm{pipe}} V_{\mathrm{pipe}} \frac{\mathrm{d}T_{\mathrm{pipe}}}{\mathrm{d}t} \tag{13}$$

$$\frac{\mathrm{d}U}{\mathrm{d}t} = q_F'' A_o - \alpha_i A_i (T_{\mathrm{pipe}} - T_{\mathrm{gas}}); \quad T_{\mathrm{gas}} = \mathrm{const.} \tag{14}$$

Resolving these two differential equations, leads to the following equations of pipe temperature over time and the second at which time critical temperature will occur:

$$T_{\text{pipe}} = T_{\text{gas}} + \frac{d_o \dot{q}''_F}{\alpha_i d_i} + \left[T_o - \left(T_{\text{gas}} + \frac{d_o \dot{q}''_F}{\alpha_i d_i} \right) \right] \text{e}^{-\frac{4\alpha_i d_i}{\rho_{\text{pipe}} c_{\text{pipe}} \, d_o^2 - d_i^2} t} \quad \text{[K]} \tag{15}$$

$$t = \frac{\rho_{\text{pipe}} c_{\text{pipe}} (d_o^2 - d_i^2)}{4\alpha_i d_i} \ln \frac{T_o - \left(T_{\text{gas}} + \frac{d_o \dot{q}''_F}{\alpha_i d_i} \right)}{T_{\text{pipe}} - \left(T_{\text{gas}} + \frac{d_o \dot{q}''_F}{\alpha_i d_i} \right)} \quad \text{[s]} \tag{16}$$

Calculation of wall temperature

The FLUENT simulation in chapter 4 shows that the maximal radiative heat flux on the pipe is $\dot{q}''_F = 9$ kW/m^2 at present boundary conditions.

It follows that all necessary initial information for resolving the last two equations are fulfilled in eqs. (15) and (16), to calculate the temperature of the wall for different time periods at constant radiation of 9 kW/m^2 and different velocities of gas inside of the pipe. Convective heat transfer coefficient was retrieved from fig. 12 for each gas velocity during calculation process. Results are shown in fig. 13.

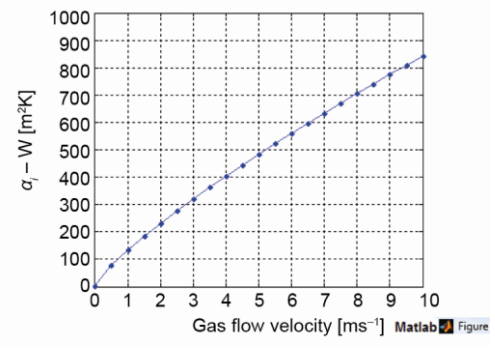

Figure 12. Change of heat transfer coefficient α_i over gas velocity inside the pipe

From fig. 13 it is clearly visible that at constant heat flux of 9 kW/m^2, there is no danger for greater incident on the pipe, because temperature of the wall cannot reach 400 °C for constant flow of gas inside the pipe. This was one of the main points in this paper to investigate and present. Further plots present possible situations for the wall temperature applying eq. (15) for different intensities of radiation $\dot{q}''_F$, different velocities of gas and after 15 minutes of combustion.

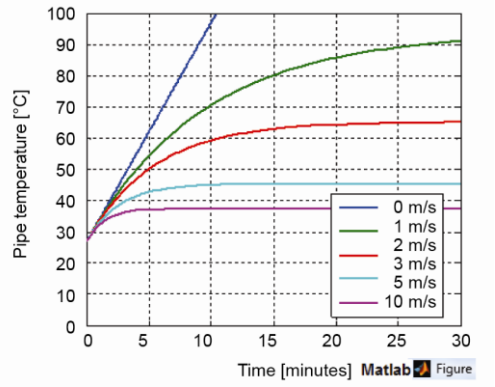

Figure 13. Pipe temperature for different times, velocities and constant radiative heat of 9 kW/m^2, internal diameter of pipe 900 mm and wall thicknes 20 mm

For practical engineers who deal with gas industry one of the most important piece of information during accidents is the thermal length of the burning gas jet. Figure 6 shows that the risk zone is up to 16-20 m where the temperature goes from 500-2250 K.

For this particular case and simulated pipe line, it is clearly visible from fig. 13 that at constant heat flux of 9 kW/m^2, there is no further danger for greater incident on the pipe, because the temperature of the wall cannot exceed 400 °C at constant flow of gas inside the pipe. From figs. 14 and 15 it is visible that further danger for grater rapture can occur only at higher incident radiation, above 50 kW/m^2.

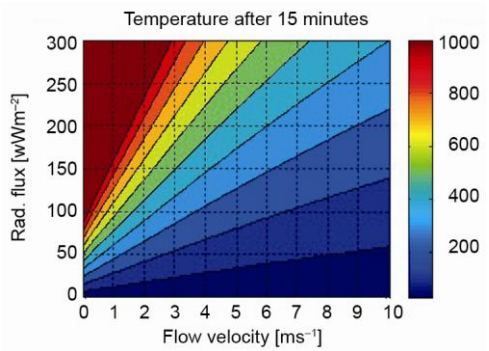

Figure 14. Pipe temperature for different heat fluxes, velocities and after 15 minutes

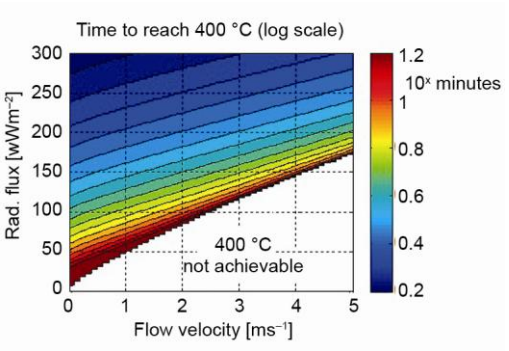

Figure 15. Time period when 400°C is achieved for different heat fluxes and velocities of gas inside of the pipe

Nomenclature

- a – optical thickness, [m]
- c_p – specific heat capacity at constant pressure, [$m^2s^{-2}K^{-1}$]
- d_i – internal diameter of pipe, [m]
- d_o – external diameter of pipe, [m]
- H – enthalpy, [m^2s^{-2}]
- $\dot{m}$ – mass flow, [kgs^{-1}]
- p – pressure, [$kgm^{-1}s^{-2}$]
- $\dot{q}''_F$ – incident radiation heat on the pipe, [Wm^{-2}]
- T – absolute temperature, [K]
- t – time, [s]
- $\vec{v}$ – velocity, [ms^{-1}]

Greek symbols

- α – convective heat coefficient [$Wm^{-2}K^{-1}$]
- λ – conduction heat coefficient [$Wm^{-1}K^{-1}$]
- χ – Poisson coefficient
- μ_t – turbulent viscosity [$kgm^{-1}s^{-1}$]
- ν – kinematic viscosity [m^2s^{-1}]
- ρ – density [kgm^{-3}]
- $\boldsymbol{\tau}$ – viscous stress tensor [$kgm^{-1}s^{-2}$]
- Ω' – radiative solid angle

Acronyms

CFD – computational fluid dynamics
RTE – radiative transport equation

References

[1] ***, API 521, *Guide for Pressure-Relieving and Depressuring Systems*, American Petroleum Institute, 1997
[2] ***, EN ISO 23251, *Petroleum, Petrochemical and Natural Gas Industries-Pressure-Relieving and Depressuring Systems*, European Committee for Standardization, 2007
[3] Keiser, W. *et al*., Ermittlung und Berechnung von Störfallblaufszenarien nach Massgabe der 3. Störfallverwaltungsvorschrift, Band 1, Technische Universität Berlin, 2006
[4] ***, User's guide, FLUENT 6.3, 2006
[5] Ouellette, P., Pressure Injection of Natural Gas for Diesel Engine Fueling, M. Sc. thesis, The University of British Columbia, Vancouver, Canada, 1992
[6] Birch, A. D. et al., The Structure and Concentration Decay of High Pressure Jets of Natural Gas (in German), *Combustion Science and Technology, 36* (1984), pp. 249-261
[7] Patankar, S. V., *Numerical Heat Transfer and Fluid Flow*, Hemisphere P. C., 1980
[8] Davenport J. N., Thermal Response of Vessels and Pipe Work Exposed to Fire, Imperial College for The Steel Construction Institute-HMSO, 1992
[9] Ilić, G., Radojković, N., Stojanović, I., *Thermodynamics II – Basics of Heat Distribution* (in Serbian), Faculty of Mechanical Engineering, University of Nis, Yugoslavia, 1996

Paper submitted: May 3, 2012
Paper revised: July 25, 2012
Paper accepted: August 8, 2012